IAHR/COPRI Symposium "Long Waves and Relevant Extremes"
E-proceedings of the 36th IAHR World Congress
28 June – 3 July, 2015, The Hague, the Netherlands

NEARSHORE COMPOUND SIMULATION BY A BOUSSINESQ-TYPE WAVE MODEL

GEORGIOS TH. KLONARIS[(1)], CONSTANTINE D. MEMOS[(2)] & CHRISTOS V. MAKRIS[(3)]

[(1)] *School of Civil Engineering, National Technical University of Athens, Zografos, Athens, Greece, gklon@hydro.ntua.gr*

[(2)] *School of Civil Engineering, National Technical University of Athens, Zografos, Athens, Greece, memos@hydro.ntua.gr*

[(3)] *Department of Civil Engineering, Aristotle University of Thessaloniki, Thessaloniki, Greece, cmakris@civil.auth.gr*

ABSTRACT

A two-dimensional, in the horizontal plane, high order Boussinesq-type model is presented to simulate wave propagation in the nearshore zone. The model is extended to the surf zone by applying a wave breaking module of the eddy viscosity type and to the swash zone by applying a modified narrow slot technique. Bottom friction and subgrid turbulent mixing are also incorporated. The numerical model relies on a generalized multi-step predictor-corrector scheme. Both the one- and two-dimensional model versions are verified with a number of experimental cases involving regular and irregular wave propagation in the nearshore. A comparison with a Smoothed Particle Hydrodynamics (SPH) model is also included. In general, the agreement is satisfactory and most of the nearshore phenomena are accurately reproduced.

Keywords: Boussinesq model; Wave breaking; SPH model; Wave run-up.

1. INTRODUCTION

During the last decades Boussinesq-type wave models have been a field of intense scientific research. In this context, the main interest of researchers has been the enhancement of the dispersive and nonlinear character of this type of models in order to be applicable to more and more deep water. Thus the nonlinear shallow water equations were initially extended by Peregrine (1967) to account for weakly dispersive waves. His "classical" Boussinesq equations provoked scientists to extend their range of applicability further offshore by enhancing their linear and nonlinear characteristics (Madsen *et al.*, 1991; Nwogu, 1993; Wei *et al.*, 1995; Madsen and Schäffer, 1998; Gobbi *et al.*, 2000). More recently, some advanced post-Boussinesq models have eliminated any virtual depth limitation (Madsen *et al.*, 2002; Karambas and Memos, 2009).

Extending inshore has been another challenge for Boussinesq models for the sake of coastal engineering applications. In order to simulate surf and swash zone dynamics, a number of complex physical processes have to be accurately reproduced. In particular, three different techniques have been mainly proposed for simulating wave breaking. The first one relies on the eddy viscosity concept (Zelt, 1991; Kennedy *et al.*, 2000), the second one on the surface roller approach (Schäffer *et al.*, 1993) and the last one employs a vorticity transport model (Veeramony and Svendsen, 2000). On the other hand, extension to the swash zone requires a treatment of the moving shoreline (Pedersen and Gjevik, 1983; Militello *et al.*, 2004).

In the present work, a 2DH higher-order Boussinesq-type model is presented to simulate wave propagation over the entire nearshore zone. Extension to the surf zone is attained by treating wave breaking through the eddy viscosity concept, while wave run-up is simulated by applying a modified slot technique. The model is validated against a number of experimental tests, both in one and two horizontal dimensions. The test cases involve regular and irregular wave propagation on plane beaches and over submerged shoals. A comparison with a modern Computational Fluid Dynamics (CFD) approach for free surface flows, implemented by Makris *et al.* (2015a; 2015b), is also presented. The latter approach is based on Smoothed Particle Hydrodynamics (SPH), a Lagrangian mesh-free (particle) method. The Boussinesq-type model's response is, in general, reasonably good proving the model's ability to adequately reproduce the above physical processes.

2. BOUSSINESQ-TYPE MODEL FORMULATION

The present model is based on one- and two-dimensional Boussinesq equations expressed in terms of depth-averaged velocity. Following Veeramony and Svendsen (2000), an enhanced version of higher order nonlinearity of Karambas and Koutitas's (2002) model was derived. The two-dimensional version of the model relies on Eqs [1]-[3]:

$$\beta \frac{\partial \zeta}{\partial t} + \nabla_{\mathrm{h}} \cdot \left(\Lambda \vec{U}\right) = 0 \qquad [1]$$

$$\frac{\partial U}{\partial t} + U\frac{\partial U}{\partial x} + V\frac{\partial U}{\partial y} + \mathrm{g}\frac{\partial \zeta}{\partial x} = \left(\mathrm{B} + \frac{1}{3}\right) d^2\left(U_{xxt} + V_{xyt}\right) + (2\mathrm{B}_2 + 1)dd_x U_{xt} + \left(\mathrm{B}_2 + \frac{1}{2}\right) dd_x V_{yt} + \left(\mathrm{B}_2 + \frac{1}{2}\right) dd_y V_{xt} + \mathrm{B}d^2\left(\zeta_{xxx} + \zeta_{xyy} + \mathrm{B}2\right) 2ddx\zeta xx + ddy\zeta xy + ddx\zeta yy + \psi Ix + \psi IIx + Fbr + \tau bxd + \zeta + Feddy + Fsp \qquad [2]$$

$\frac{\partial V}{\partial t} + U\frac{\partial V}{\partial x} + V\frac{\partial V}{\partial y} + \mathrm{g}\frac{\partial \zeta}{\partial y} = \left(\mathrm{B} + \frac{1}{3}\right) d^2\left(V_{yyt} + U_{xyt}\right) + (2\mathrm{B}_2 + 1)dd_yV_{yt} + \left(\mathrm{B}_2 + \frac{1}{2}\right) dd_yU_{xt} + \left(\mathrm{B}_2 + \frac{1}{2}\right) dd_xU_{yt} + \mathrm{B}d^2(\zeta_{yyy} + \zeta xxy + \mathrm{B}2\,2ddy\zeta yy + ddx\zeta xy + ddy\zeta xx + \psi Iy + \psi IIy + Gbr + \tau byd + \zeta + Geddy + Gsp$ [3]

where *t* is the time, (x, y) denote the horizontal dimensions, $\nabla_\mathrm{h} = \left(\frac{\partial}{\partial x}, \frac{\partial}{\partial y}\right)$ is the horizontal gradient operator, ζ is the free surface elevation, $\vec{U} = (U, V)$ the depth-averaged horizontal velocity, *d* the still water depth, g the gravitational acceleration, B and B_2 free parameters. The Boussinesq terms $\psi_I^{(x)}, \psi_I^{(y)}$ and $\psi_{II}^{(x)}, \psi_{II}^{(y)}$ are of $O(\varepsilon\sigma^2)$ and $O(\varepsilon^2\sigma^2)$ respectively, where $\varepsilon = H/d_0$ is the nonlinearity parameter and $\sigma^2=(d_0/L)^2$ is the dispersion parameter with *H*, d_0 and *L* a reference wave height, water depth and wavelength, respectively. Their lengthy expressions can be found in Klonaris *et al.* (2015). The terms F_{br} and G_{br} account for the wave breaking, τ_{bx} and τ_{by} for the bottom friction stresses and F_{eddy} and G_{eddy} for the subgrid turbulent mixing. Finally, F_{sp} and G_{sp} are damping terms applied to absorb the energy of the outgoing waves as described in Section 3.

The parameters $\beta = \beta(\zeta)$ and $\Lambda = \Lambda(\zeta)$ result from the application of a slot technique to simulate wave run-up and run-down. The present wave model simulates the wave motion in the swash zone following the procedure described by Kennedy *et al.* (2000) and Chen *et al.* (2000). This is basically a modification of the slot method originally proposed by Tao (1983, 1984). The main idea is that, instead of tracking the moving boundary, the entire computational domain is considered active, but wherever there is very little or no water covering the land, modified equations are being solved. These equations assume that, the beach, instead of being solid, contains narrow 'slots', so that it be possible for the water level to be below the beach elevation. Hence the shoreline is at any instant determined by the intersection of the water surface and the sea bed.

This modified slot method ensures that, there is no net fluid loss at a specific location when water is above the top of the slot in contrary to the original method of Madsen *et al.* (1997a; 1997b). However, some small, but much reduced, mass loss still exists when water level is below the top of the slot. The parameters β and Λ are defined by:

$$\beta(\zeta) = \begin{cases} 1, & \zeta > z^* \\ \delta + (1-\delta)e^{\lambda(\zeta - z^*)/\mathrm{h_o}}, & \zeta \le z^* \end{cases} \quad [4]$$

$$\Lambda(\zeta) = \begin{cases} (\zeta - z^*) + \delta(z^* + \mathrm{h_o}) + \frac{(1-\delta)\mathrm{h_o}}{\lambda}\left[1 - e^{-\lambda(1+z^*/\mathrm{h_o})}\right], & \zeta > z^* \\ \delta(\zeta + \mathrm{h_o}) + \frac{(1-\delta)\mathrm{h_o}}{\lambda}e^{\lambda(\zeta - z^*)/\mathrm{h_o}}\left[1 - e^{-\lambda(1+\zeta/\mathrm{h_o})}\right], & \zeta \le z^* \end{cases} \quad [5]$$

where δ is the slot width relative to a unit width of the beach, λ is the shape parameter that controls the smooth transition of the cross-sectional area from a unit width to a narrow slot, $\mathrm{h_o}$ is the water depth at the offshore end of the slot and z^* denotes the elevation of the sea bed where $\beta = 1$ given by:

$$z^* = \frac{-d}{1-\delta} + \mathrm{h_o}\left(\frac{\delta}{1-\delta} + \frac{1}{\lambda}\right) \quad [6]$$

In all of the applications presented here the values λ = 80 and δ = 0.001÷0.01 were applied.

The model was extended into the surf zone by incorporating wave breaking based on the eddy viscosity concept described by Kennedy *et al.* (2000). The breaking terms are expressed as:

$$F_{br} = \frac{1}{d+\zeta}\left\{\{v_{br}[(d+\zeta)U]_x\}_x + \frac{1}{2}\left\{v_{br}[(d+\zeta)U]_y + v_{br}[(d+\zeta)V]_x\right\}_y\right\} \quad [7]$$

$$G_{br} = \frac{1}{d+\zeta}\left\{\left\{v_{br}[(d+\zeta)V]_y\right\}_y + \frac{1}{2}\left\{v_{br}[(d+\zeta)V]_x + v_{br}[(d+\zeta)U]_y\right\}_x\right\} \quad [8]$$

where v_{br} is the eddy viscosity coefficient localized on the front face of the breaking wave as:

$$v_{br} = B_{br}\delta_\mathrm{b}^2(d+\zeta)\zeta_t \quad [9]$$

with the mixing length coefficient set equal to $\delta_\mathrm{b} = 1.2$ and the quantity B_{br} given by:

$$B_{br} = \begin{cases} 1, & \zeta_t \ge 2\zeta_t^* \\ \frac{\zeta_t}{\zeta_t^*} - 1, & \zeta_t^* < \zeta_t < 2\zeta_t^* \\ 0, & \zeta_t \le \zeta_t^* \end{cases} \quad [10]$$

The parameter ζ_t^* determines the onset and cessation of breaking as:

$$\zeta_t^* = \begin{cases} \zeta_t^{(F)}, & t - t_0 \geq T^* \\ \zeta_t^{(I)} + \frac{t-t_0}{T^*}\left(\zeta_t^{(F)} - \zeta_t^{(I)}\right), & 0 \leq t - t_0 < T^* \end{cases} \quad [11]$$

where $T^* = 5\sqrt{d/\mathrm{g}}$ is the transition time from breaking initiation to a fully developed bore and t_0 is the time that breaking was initiated. A typical value of $\zeta_t^{(F)}$ is $0.15\sqrt{\mathrm{g}d}$, while parameter $\zeta_t^{(I)}$ varies from $0.35\sqrt{\mathrm{g}d}$ for bar/trough beaches to $0.65\sqrt{\mathrm{g}d}$ for monotonic sloping beaches.

The model offers two options for computing the bed shear stresses. The first one is using a quadratic resistance law for the instantaneous stresses:

$$\vec{\tau}_b = \left(\tau_{bx}, \tau_{by}\right) = \tfrac{1}{2} f_{cw} \vec{U}\left|\vec{U}\right| \quad [12]$$

where f_{cw} is the bed friction coefficient that is typically a function of both the wave and the current fields. A detailed description for the estimation of the bed friction coefficient can be found in Rakha *et al.* (1997) and Memos *et al.* (2005). Besides this analytical computation, a value of f_{cw}, constant in each run, lying in the range 0.001÷0.01 was also employed here for simplicity reasons leading to acceptable results.

An alternative formulation relies on the more sophisticated probabilistic analysis by Kobayashi *et al.* (2007). Assuming equivalence between time and probabilistic averaging as well as a Gaussian distribution of the oscillatory horizontal velocity with zero mean, the bed stresses can be approximated by:

$$\vec{\tau}_b = \left(\tau_{bx}, \tau_{by}\right) = \tfrac{1}{2} f_{cw} \sigma_T^2 \left(G_{bx}, G_{by}\right) \quad [13]$$

where σ_T is the standard deviation of the oscillatory horizontal velocity with zero mean given by:

$$\sigma_T = \left[g\left(d + \bar{\zeta}\right)\right]^{0.5} \sigma_* \quad [14]$$

with $\sigma_* = \sigma_\zeta / (d + \bar{\zeta})$ and $\bar{\zeta}$, σ_ζ the mean value, the standard deviation of the free surface elevation ζ, respectively. Normally, $\left(G_{bx}, G_{by}\right)$ are improper integrals of functions of the velocity field. However, the simplified expressions by Feddersen *et al.* (2000) were used here leading to acceptable deviations:

$$G_{bx} = \frac{\bar{U}}{\sigma_T}\left[1.16^2 + \left(\frac{\bar{U}}{\sigma_T}\right)^2\right]^{0.5} \text{ and } G_{by} = \frac{\bar{V}}{\sigma_T}\left[1.16^2 + \left(\frac{\bar{V}}{\sigma_T}\right)^2\right]^{0.5} \quad [15]$$

with $\vec{\bar{U}} = (\bar{U}, \bar{V})$ the current velocity field described below. For the applications presented here both formulations led to quite similar results. Hence no clear evidence emerged proving the superiority of either approach.

Due to the complex three-dimensional nature of the turbulence an approximation was applied. In particular, as this Boussinesq model is based on vertically integrated mass and momentum equations and the grid size is usually smaller than the typical depth, the concept of Large Eddy Simulation was applied on the horizontal plane to parameterize a good portion of the effects of unresolved small-scale motions. The effects of subgrid turbulent processes on the horizontal plane were thus taken into account by using the Smagorinsky-type subgrid model (Chen *et al.*, 1999; Zhan *et al.*, 2003) which yields the following extra terms:

$$F_{eddy} = \frac{1}{d+\zeta}\left\{\{v_e[(d+\zeta)U]_x\}_x + \frac{1}{2}\left\{v_e[(d+\zeta)U]_y + v_e[(d+\zeta)V]_x\right\}_y\right\} \quad [16]$$

$$G_{eddy} = \frac{1}{d+\zeta}\left\{\left\{v_e[(d+\zeta)V]_y\right\}_y + \frac{1}{2}\left\{v_e[(d+\zeta)V]_x + v_e[(d+\zeta)U]_y\right\}_x\right\} \quad [17]$$

where v_e is the eddy viscosity coefficient due to the subgrid turbulence estimated by:

$$v_e = \mathrm{c_s}\,\mathrm{d}x\,\mathrm{d}y\left[\bar{U}_x{}^2 + \bar{V}_y{}^2 + \tfrac{1}{2}\left(\bar{U}_y + \bar{V}_x\right)^2\right]^{1/2} \quad [18]$$

in which c_s is the mixing coefficient with a default value of 0.25 and $\mathrm{d}x$ and $\mathrm{d}y$ are the grid spacing in the x and y directions, respectively.

The traditional treatment of nearshore dynamics requires splitting of the total flow field into a wave and a current problem. The decoupled approach includes at first the computation of the radiation stresses from a wave model and then the solution of the nonlinear shallow water equations for the mean flow driven by them. This practice is both time consuming and more importantly it omits the wave-current interaction. However, this decoupled procedure is not needed for a nonlinear Boussinesq-type model, as this one, when it be extended to the surf and swash zones (Basco, 1983). These models provide inherently the combined effects of wave-wave and wave-current interactions, without the need of explicit formulation for the radiation stresses.

The total horizontal velocity, $\vec{u} = \vec{u}(x, y, z, t)$, with z the vertical coordinate, can be written as the sum of a mean velocity, $\vec{\overline{U}} = (\bar{U}, \bar{V})$ assumed uniform over depth, and an oscillatory component, $\vec{u}_w$. The depth-averaged mean horizontal velocity is introduced in such a way that if multiplied by the mean water depth gives the mean mass flux (Mei, 1983; Dingemans, 1994). The horizontal mean velocity, $\vec{\overline{U}}$, so defined has actually two components, the wave-induced current field plus the effect of the mass flux due to the wave motion, i.e. it includes the Stokes drift.

It should be noted that the one-dimensional version of the model reduces to Karambas and Koutitas's (2002) model if term $\psi_{II}^{(x)}$ (or $\psi_{II}^{(y)}$) is omitted in Eq. [2] (or Eq. [3]). Thus, the present model offers an enhancement of the nonlinear properties of their equations, especially concerning the nonlinear amplitude dispersion. For a comprehensive study on this issue see Memos *et al.* (2015) and Klonaris *et al.* (2015). The values B = 1/15 and B_2 = 0.0653 give the minimum error for the linear dispersion and linear shoaling gradient (Madsen *et al.*, 1991; Schäffer and Madsen, 1995) and were adopted herein.

3. NUMERICAL MODEL

The differential Eqs [1]-[3] were solved numerically using a finite difference scheme on a non-staggered grid. Terms involving first-order spatial derivatives were differenced to $O(\Delta x^4)$ while second and third-order spatial derivatives were differenced to $O(\Delta x^2)$. This was chosen in order to reduce the truncation errors to a small amount relative to each of the retained terms in the equations.

Time integration is performed using a generalized multi-step predictor-corrector scheme proposed by Zlatev *et al.* (1984). The predictor formula is of the third order, followed by a fourth-order corrector arrangement. The corrector step was iterated if the relative error between two successive results exceeded 0.001. For weakly nonlinear waves the scheme required typically no iterations, unless problems arose from the boundaries. However, for strong nonlinear problems, more iterations were required. In order to increase the convergence rate, a relaxation technique was applied at the corrector stage. Numerical instabilities were removed in most of the cases by applying a fourth-order Shapiro (1970) numerical filter.

The desired waves were generated inside the computational domain by introducing a source term in the continuity Eq. [1]. The analytical expression for this source function term is given in Klonaris *et al.* (2015). The basic idea behind this method is the distribution of the source function over a certain neighbourhood of the source in order to avoid the generation of spurious noise around the source point (Wei *et al.*, 1999).

For a reflective boundary with an outward normal vector $\vec{n}$, three conditions were imposed :

$$\vec{U} \cdot \vec{n} = 0 \ , \ \nabla_h \zeta \cdot \vec{n} = 0 \ , \ \frac{\partial \vec{U}_T}{\partial \vec{n}} = 0 \ , \ \forall \ \vec{x} \in \partial\Omega \qquad [19]$$

where Ω is the fluid computational domain, $\partial\Omega$ is the reflective boundary of the associated domain, $\vec{x}$ is a position in the domain and $\vec{U}_T$ is the velocity component tangent to the boundary.

Absorbing boundary conditions yield extra damping terms, F_{sp} and G_{sp} in Eqs [2] and [3] given by:

$$F_{sp} = -\alpha_1 \omega f(x) U - \alpha_2 \nu_{sp} f(x) \left(U_{xx} + U_{yy}\right) \qquad [20]$$

$$G_{sp} = -\alpha_1 \omega f(x) V - \alpha_2 \nu_{sp} f(x) \left(V_{xx} + V_{yy}\right) \qquad [21]$$

for a sponge layer parallel to the y-axis. The constants $\alpha_1, \alpha_2, \nu_{sp}$ are determined for each specific run, ω is the frequency of the wave to be damped and $f(x)$ is a relaxation function varying smoothly from 0 to 1 (Israeli and Orszag, 1981; Wei and Kirby, 1995).

4. MODEL VERIFICATION

Both the 1DH and 2DH model versions were verified against a number of experimental tests involving both regular and irregular wave propagation. Some of the tests were very demanding since they addressed simultaneously a number of physical processes such as shoaling, depth refraction, diffraction, breaking, wave run-up and nonlinear energy transfer. A comparison against the results of an SPH simulation with refined spatial resolution is also presented.

4.1 1DH verification

4.1.1 Regular breaking waves on a planar beach

The first test refers to the experiment by Hansen and Svendsen (1979) involving shoaling and breaking regular waves in a wave flume. The waves were generated on a horizontal bottom at a depth of 0.36 m, followed by a planar beach of slope 1:34.26. The test case presented here is No. 051041 involving spilling breaking waves with a period of T = 2 s and incoming wave height H_0 = 0.036 m. A comparison between the measured and the computed wave height and wave setup is shown in Figs 1 and 2, respectively.

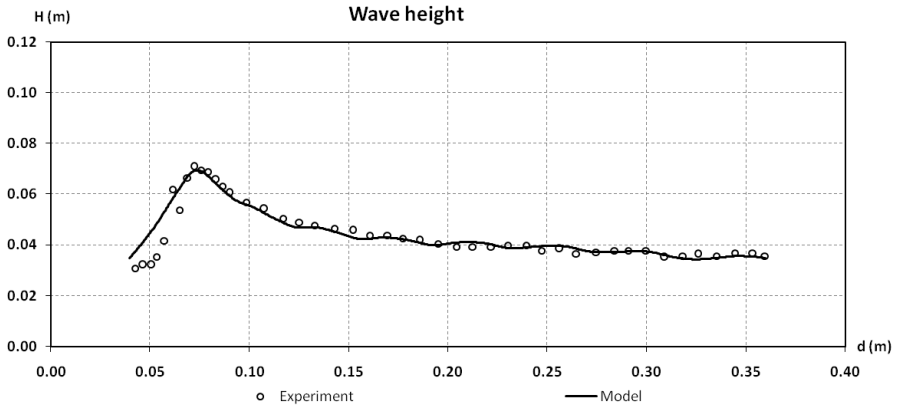

Figure 1. Computed and measured wave height for spilling breaker case No. 051041.

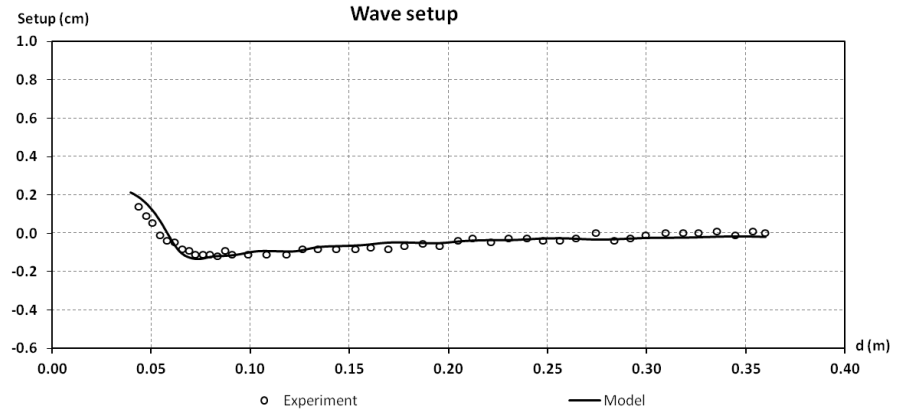

Figure 2. Computed and measured wave setup for spilling breaker case No. 051041.

The dimensionless wavenumber in the source region was kd = 0.64 which is lying in the range of applicability of the present model ($kd \leq 3$). The comparison is very good since both the breaking height and the initiation of breaking are well-predicted. There is only a slight over-prediction of wave height and setup in the inner surf zone. This has been also observed in other Boussinesq-type models simulating wave breaking by using the eddy viscosity breaking module (Kennedy *et al*., 2000).

4.1.2 Solitary wave breaking and run-up

In order to further check the model's response in the surf and swash zones the experiment by Synolakis (1987) was simulated. This corresponds to the propagation and breaking of a solitary wave on a laboratory beach of constant slope 1:19.85. Waves were generated at a distance 14.68 m offshore from the toe of the slope. The beach consisted of a ramp made out of anodized aluminium panels with a hydrodynamically smooth surface. Thus in the numerical simulations bed friction was neglected. The still water depth in the constant depth region was d = 0.2 m and the wave height H = 0.056 m giving a ratio H/d=0.28. In Fig. 3 a comparison is shown between experimental data and snapshots of the non-dimensional surface elevation ζ/d as computed from the model at different non-dimensional times $t' = t\sqrt{g/d}$.

The model's response to this demanding test was quite good both in the surf and swash zones. The nonlinear steepening is well-reproduced until the inception of breaking, i.e. around t'=20. The almost vertical wave front is very accurately described, and so is the breaking wave form in the surf zone. In addition, the moving shoreline concept behaved well, except for a slightly thinner wave tongue during the downwash as expected (see discussion in Section 2). A slight over-estimation of the maximum run-up could be possibly attributed to the neglect of the bed friction. Nevertheless, the simulation of run-up and run-down stages are generally acceptable.

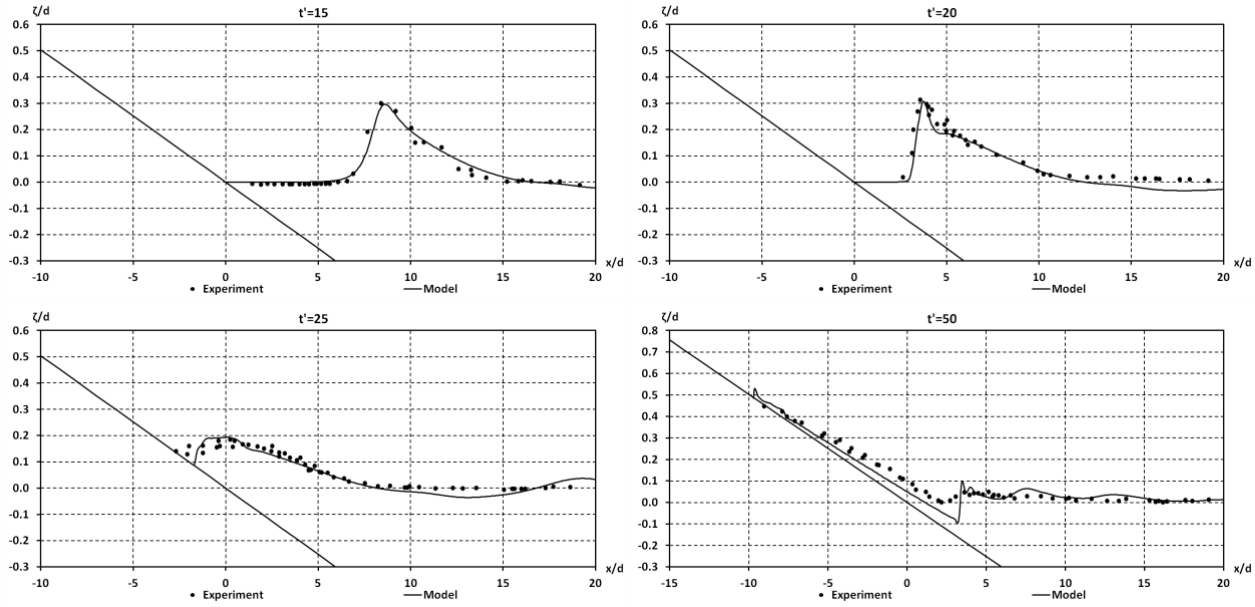

Figure 3. Measured and computed snapshots of the solitary wave run-up in Synolakis's (1987) experiment.

4.1.3 Irregular wave breaking over a submerged bar

Another test for the verification of the one-dimensional model corresponds to irregular waves propagating and breaking over a submerged trapezoidal bar. The experimental layout was the one used by Beji and Battjes (1994) and is depicted in Fig. 4. The specific test simulated here corresponds to random waves of a Jonswap spectrum, generated on a horizontal bottom of depth 0.4 m. The peak period was T_p = 2 s and the dominant breaker over the bar was of the spilling type.

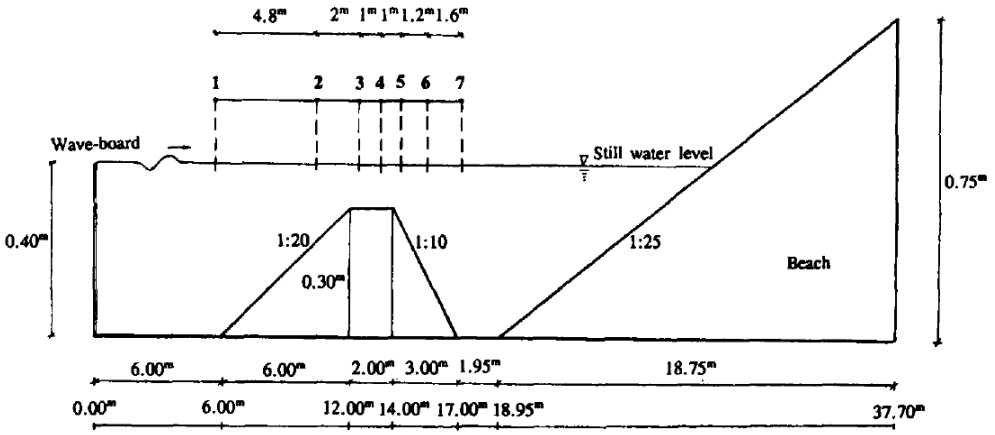

Figure 4. Layout of Beji and Battjes's (1994) experiment (from Beji and Battjes, 1994).

Wave spectra were computed from both the measured and the model's surface elevation time series. A comparison between the two is shown in Fig. 5 at four wave gauges. Although this is a quite demanding test, the model's response is reasonably good. Spectral transformation due to shoaling is very accurately reproduced for the main part of the spectrum around the peak frequency. The energy dissipation due to breaking seems reasonably predicted as the spectrum shape is described correctly and a secondary peak is formed due to wave-wave interactions. However, both the primary and the secondary peaks are over-estimated at station 5. On the other hand, the spectral density is under-predicted at the high-frequency domain. On the contrary, both the bound sub-harmonics and the released long waves due to the surf beat mechanism are computed quite accurately.

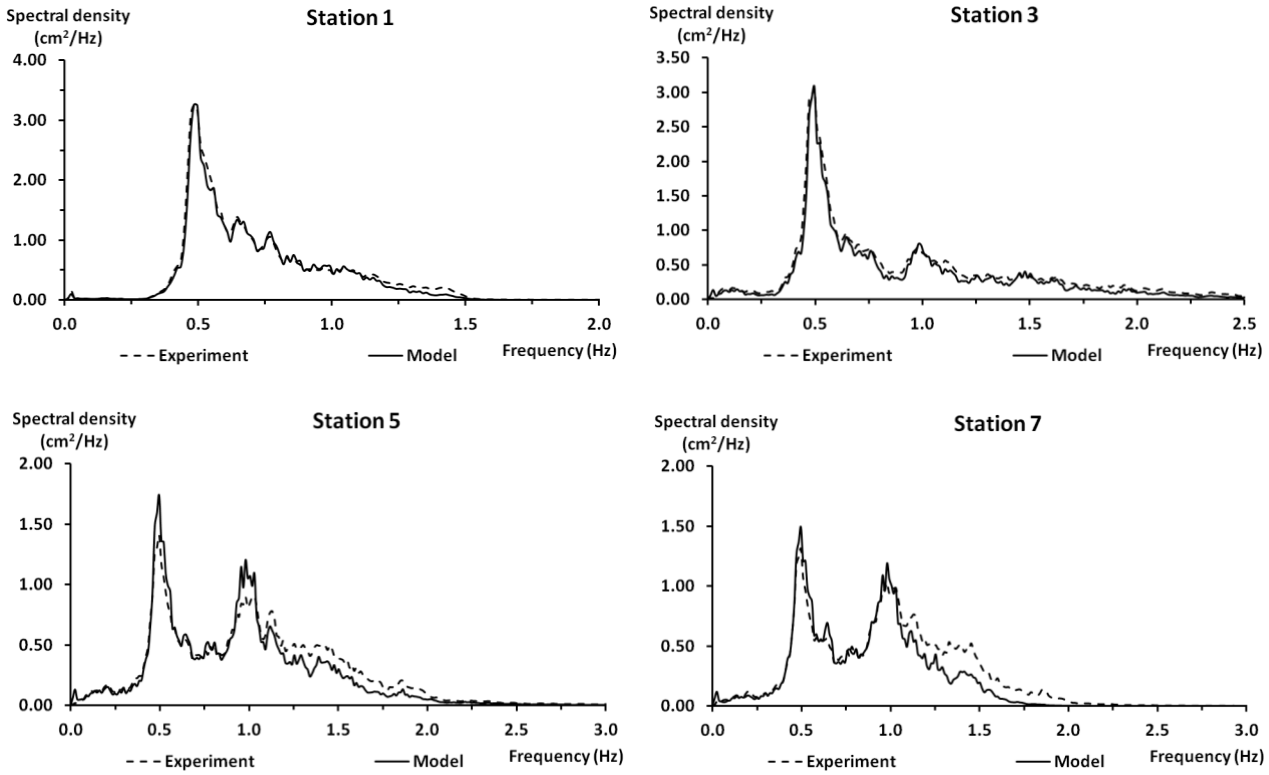

Figure 5. Measured and computed wave spectra at various wave gauges for Beji and Battjes's (1994) experiment.

4.1.4 Comparison with an SPH model against experimental data

A gridless approach, namely the SPH method (Monaghan, 2005), was also introduced for intercomparisons against the Boussinesq-type model. SPH is a mesh-free particle method, implementing spatial interpolations over all the movable nodes of the computational domain, by using integral smoothing functions for the Navier-Stokes equations written in Lagrange-type notation. It has been used extensively in the recent past for the simulation of free-surface flows with strong deformations, such as wave breaking of the plunging type in coastal areas (e.g. Dalrymple and Rogers, 2006). The method's fundamental principle is the integral interpolation of any given (scalar or vectorial) function $A(\vec{r})$ and/or its derivative in the computational domain that reads in discretized notation, as (Violeau, 2012):

$$A(\vec{r}) = \int A_j(\vec{r})\, W(\vec{r}-\vec{r}', h)\, d\vec{x} \Rightarrow A_i(\vec{r}) = \sum_j A_j\left(m_j/\rho_j\right) W_{ij} \Rightarrow \nabla A_i = \sum_j A_j\left(m_j/\rho_j\right) \nabla_i W_{ij} \quad [22]$$

where $h=c_f[(\Delta x)^2+(\Delta z)^2]^{1/2}$ is the smoothing length in 2-D, Δx and Δz are the horizontal and vertical initial spatial discretization steps respectively, c_f is a smoothing calibration parameter, $\vec{r}$ and $\vec{r}'$ are the arbitrary particle location and the distance between particles respectively, $W(\vec{r}, h)$ is the distance-varied weighting function called "kernel", *i* corresponds to an arbitrary particle (center of SPH interpolations) and *j* to particles within the compact support region of the kernel of particle *i*, m_j and ρ_j are the mass and density of particle *j* and W_{ij} is the kernel in particle notation.

Specifically a state-of-the-art vertically 2-D SPH model is implemented, in the framework of the academic 'open source' numerical code SPHysics v.2 (Gómez-Gesteira *et al*., 2010a; 2010b). The solid walls of the computational domain were treated as repulsive, which defined a more or less slip boundary condition at the inviscid limit (Gómez-Gesteira *et al*., 2010a). The symplectic time-integration technique with variable time step (Gómez-Gesteira *et al*., 2010b) was preferred for quicker simulation times. Similarly to the pseudo-LES approach in the Boussinesq-type model, a sub-particle scale (SPS) approach (Appendix of Gómez-Gesteira *et al*., 2010b) for approximate turbulence closure was incorporated, yet on a vertical plane, accounting actually for internal friction effects in terms of the stress tensor (in Einstein notation):

$$\tau_{ij} = \bar{\rho}\left[2\nu_t \tilde{S}_{ij} - 2\left(\nu_t k_{SPS}\delta_{ij} + C_l \Delta l^2 \delta_{ij}\left|\tilde{S}_{ij}\right|^2\right)/3\right],\ \nu_t = [\min(C_s \Delta l)]^2\left|\tilde{S}_{ij}\right| \quad [23]$$

where ν_t is the turbulent eddy viscosity, C_l = 0.0066, Δl is the inter-particle spacing, δ_{ij} is the Kronecker delta, k_{SPS} is the SPS turbulent kinetic energy, and $\left|\tilde{S}_{ij}\right|$ is the local strain rate calculated from the resolved variables, i.e. the norm of the second-order invariant of the Favre-filtered strain rate tensor. Hence, the eddy viscosity assumption (Boussinesq approximation) was employed in the framework of a standard, non-dynamic Smagorinsky model with a constant coefficient C_s=0.145 both in space and time, fitting the case of weak plunging breakers (Makris *et al*., 2015a).

Both the SPH and the Boussinesq-type models were applied to simulate Stansby and Feng's (2005) experiment. The specific test involves regular wave breaking of weak plunging type on a constant slope 1:20. Shorenormal waves with height H_o = 0.105 m and period T = 2.42 s were generated at a constant depth region of d = 0.34 m. A very fine spatial resolution was applied for the vertically 2-D SPH simulation, with an initial discretization step of Δx=0.001 m, requiring a variable time step of about $\Delta t = 10^{-6} \div 10^{-5}$ s. This extremely small value was chosen following the flow scale analysis by Makris *et al.* (2015a; 2015b), in order to fulfill the requirement of Δx being obviously and marginally smaller than λ_0 and $\Lambda_{EI}=\lambda_0/6$ (Pope, 2000). The latter are, in respective order, the characterisitic values of integral turbulence length scales and the demarcation point between anisotropic large eddies and isotropic small eddies. The defining λ_0 values were experimentally measured for intensely spilling breakers by Cox *et al*. (1994), and corresponded to the mixing length in the surf zone. This led to simulations engaging nearly 1.8 million particles, and it took nearly six months for the completion of a single run! Yet it was considered necessary in order to render the 2-D Smagorinsky-type SPS model active, thus incorporating a pseudo-LES implementation for SPH, i.e. by explicitly simulating the largest structures of the flow. The refinement of particle resolution to such a degree has been proven to lead to a drastic improvement of the model's results (Makris *et al.*, 2015b). On the other hand, in the Boussinesq-type model a far coarser spatial step of 0.04 m and a time step of 0.005 s were chosen for numerical stability reasons. A comparison between the measured and computed by both models wave height and wave setup is shown in Fig. 6.

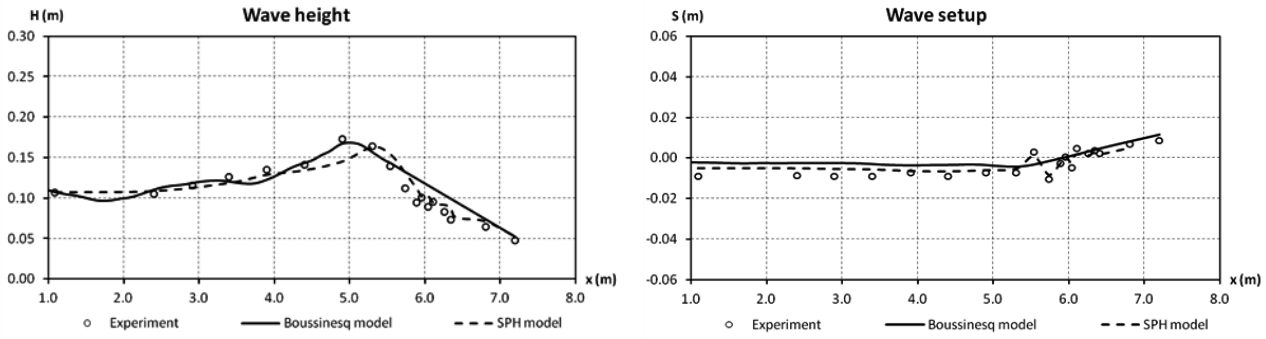

Figure 6. Measured and computed from Boussinesq-type and SPH models wave height (left) and wave setup (right) for Stansby and Feng's (2005) experiment.

Wave breaking initiation was observed at about x = 4.95 m. The wave characteristics are very accurately computed by the SPH model, especially in the surf zone. Only a slight over-estimation of the wave set-down is observed offshore. These results were expected due to the nature of this approach and the very fine grid used. They are definitely superior to the ones from the Boussinesq-type model which over-estimates the wave height in the inner surf zone. This result has been also observed in other models simulating wave breaking through the eddy viscosity concept. However, it should be noted that the specific experimental test hardly lies in the range of applicability of the specific Boussinesq-type model due to the high Ursell number, Ur = 48.19, much higher than 32 which is approximately a typical limit for the original Boussinesq theory. In addition, plunging breaking is difficult to be simulated by a Boussinesq model because total flow disruption and intense foaming take place. Thus, despite the discrepancies observed in Fig. 6 the overall response of the Boussinesq-type model to this demanding test was acceptable. Finally, it is worth mentioning that the computational time of the SPH model is more than two orders of magnitude greater than the corresponding of the Boussinesq-type model.

4.2 2DH verification

4.2.1 Regular wave propagation over an elliptic shoal

The first test for checking the validity of the two-dimensional Boussinesq-type model is the benchmark test by Berkhoff *et al.* (1982). Their experiment referred to monochromatic wave propagation over an elliptic shoal and combined a number of physical processes, such as shoaling, refraction, diffraction and nonlinear dispersion. Nonbreaking regular waves of period T = 1 s and wave height H_o = 0.0464 m were generated in a constant depth region of d = 0.45 m and propagated over an uneven bottom. The experimental layout and the bathymetry are shown in Fig. 7 (at left). The bathymetry displays an elliptic shoal resting on a 1:50 plane sloping seabed. The entire slope is turned at an angle of -20° with respect to the wave paddles.

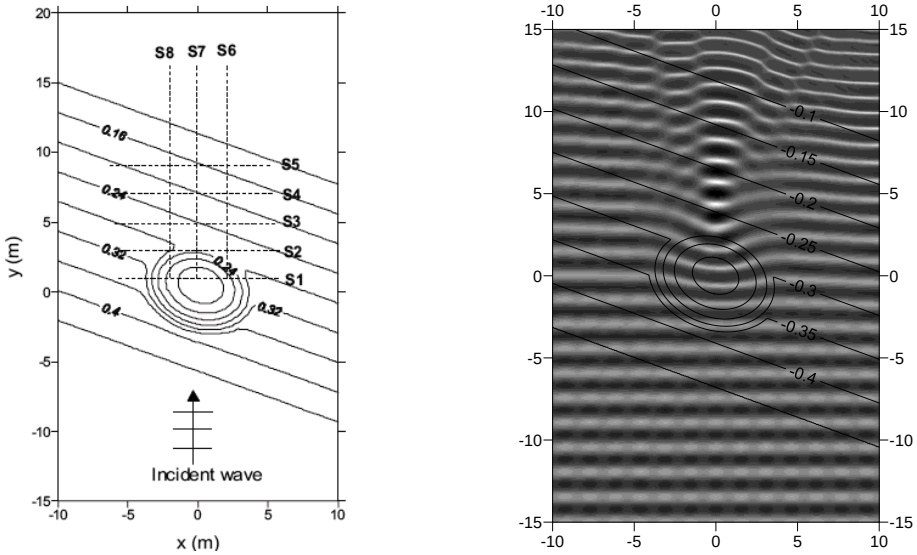

Figure 7. Left: Experimental layout and bathymetry of Berkhoff *et al.*'s (1982) experiment (contours in meters). Right: Snapshot of the free surface elevation, viewed in plan.

The computed wave field reached a stable state after t = 30 s. A snapshot of the free surface elevation at t = 40 s is also depicted in Fig. 7 (at right) in a plan view. Strong energy focus is observed behind the shoal, pronouncing the large effect of wave diffraction. Fig. 8 shows a comparison between the measured and computed wave heights along four sections of Fig. 7 (left).

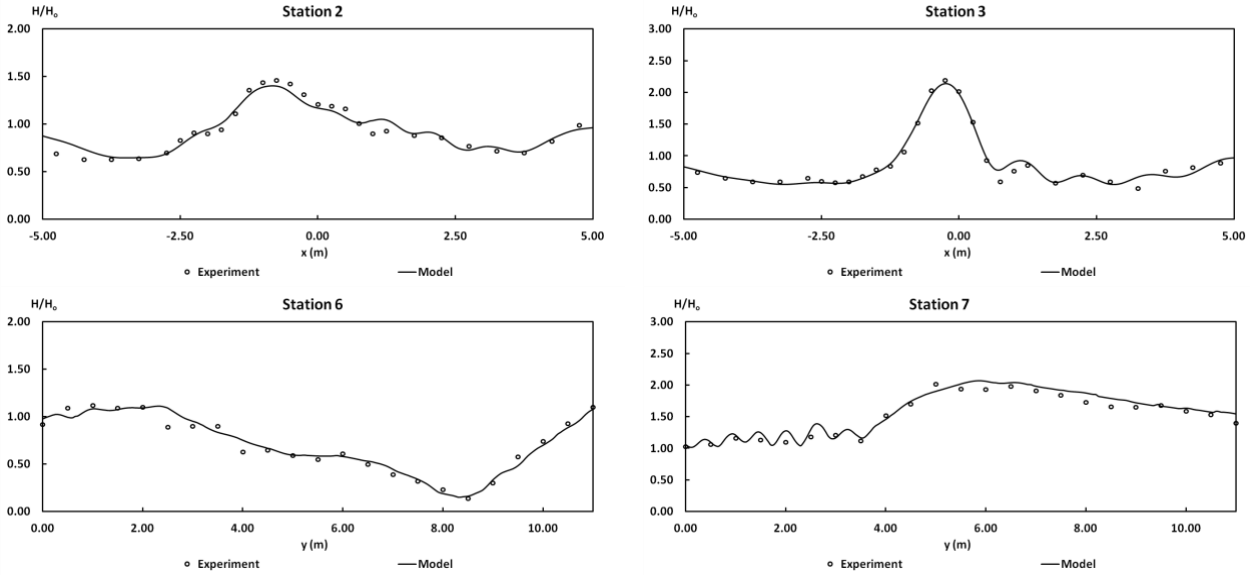

Figure 8. Computed and measured relative wave heights along four sections in Berkhoff *et al.*'s (1982) experiment.

The computed results for the wave height agree quite well with the measured ones along both directions, parallel and normal to wave incidence. The quite large values of the dimensionless wavenumber ($kd \approx 1.9$ close to the wavemaker) prove the model's ability to reproduce fairly good the nonlinear dispersion effect.

4.2.2 Oblique long-crested irregular waves

The last validation test refers to the laboratory experiments performed in the U.K. Coastal Research Facility at HR Wallingford (Memos *et al.*, 2005), aimed at studying various aspects of random wave propagation in shallow water. The basin of the facility, with overall dimensions 27 m × 54 m (Fig. 9), contained a narrow strip of horizontal bed and a rigid beach sloping uniformly at 5%. The water depth over the horizontal bed was 0.80 m. The bed was constructed rough, everywhere but for the part of the horizontal bottom between the left lateral wall and the centre line in Fig. 9, where the bed was considered smooth.

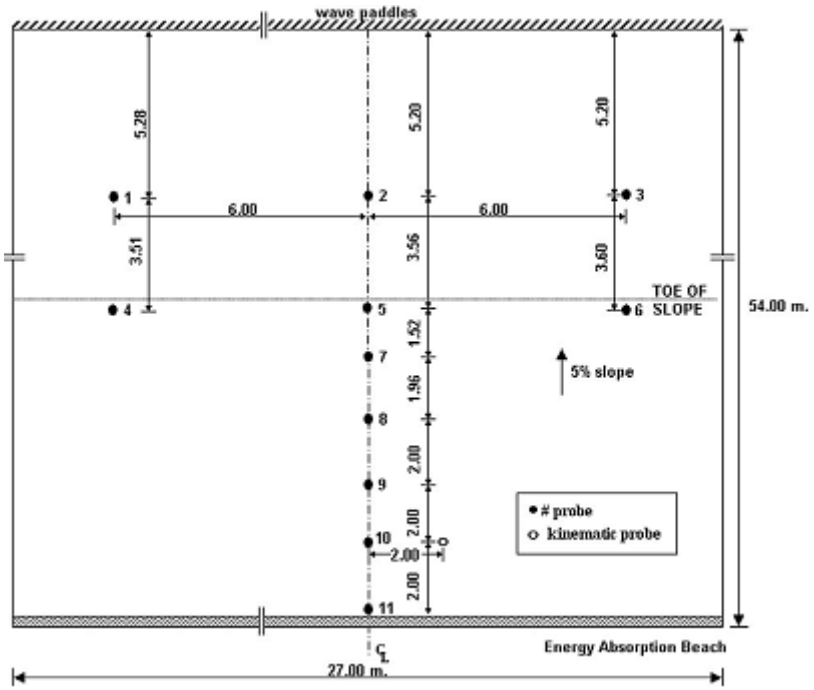

Figure 9. Plan of the experimental setup at HR Wallingford.

The test case presented herein corresponds to oblique long-crested irregular waves of a Jonswap spectrum with enhancement factor γ = 3.3, peak period T_p = 1.2 s and significant wave height at the wave paddles H_s = 0.09 m. The angle of incidence was 15° to the shore. A comparison between the wave spectra estimated from the measured and the computed surface elevation time series is depicted in Fig. 10.

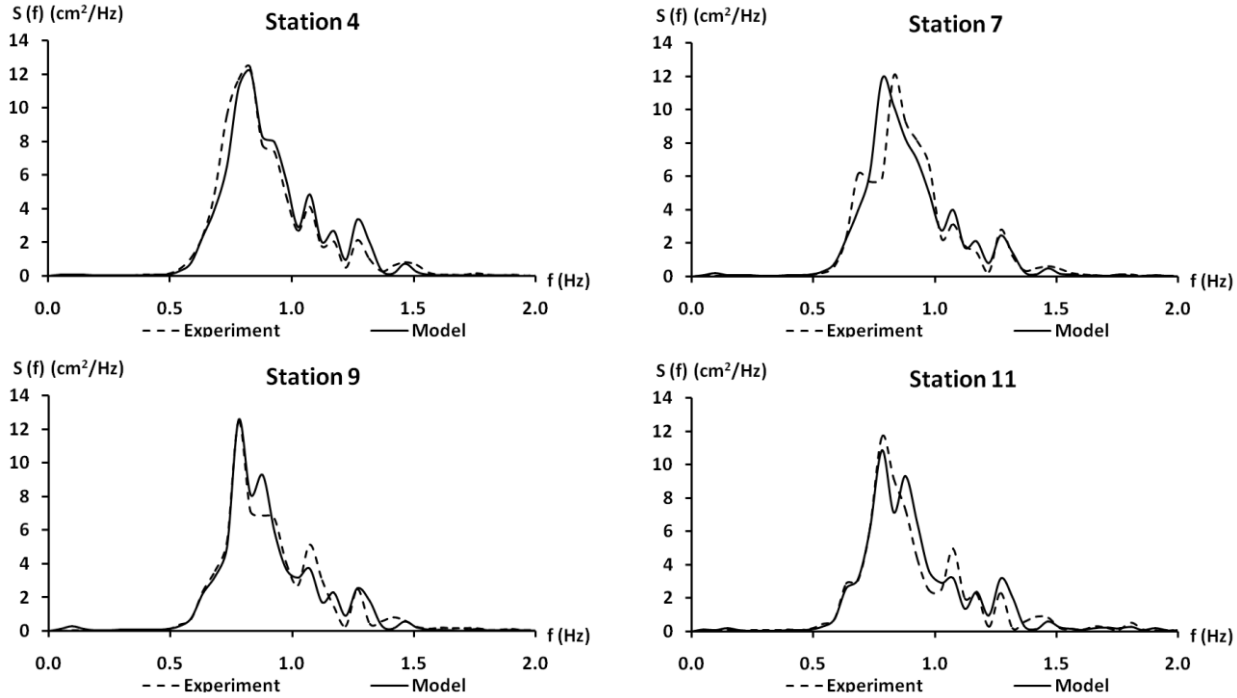

Figure 10. Measured and computed wave spectra at various wave gauges of the experiment at HR Wallingford.

The agreement seems satisfactory over a wide depth range since the corresponding to the peak frequency dimensionless wavenumber at the source area is $kd \approx 2.3$ whereas at station 11 $kd \approx 1.1$. The spectrum shape all over the wave tank and the effect of energy transfer to higher frequencies are simulated reasonably well by the present Boussinesq-type model.

5. CONCLUSIONS

A one- and two-dimensional higher-order Boussinesq-type model was presented embedding enhanced nonlinear characteristics compared to its predecessor counterpart of weaker nonlinearity. In order to form a robust tool applicable to the entire nearshore zone the major coastal physical processes have to be modelled realistically. Wave breaking was

incorporated by applying the eddy viscosity concept. However, in some cases this approach over-estimates the wave height in the inner surf zone. Wave run-up was simulated using a modified slot technique which is slightly better than the conventional one in terms of mass conservation. Bed friction was modelled using either the conventional quadratic law or a more sophisticated probabilistic method. However, both approaches led to similar results. The unresolved small-scale motions were approximated by employing a quasi-Large Eddy Simulation technique. The numerical model relies on a fourth-order generalized multi-step predictor-corrector scheme. Waves were generated by applying the source function technique, while the outgoing energy was absorbed by suitable damping layers.

The one-dimensional version of the model was applied to simulate regular wave breaking on a plane beach with very satisfactory results. Breaking and run-up of a solitary wave were also simulated fairly well, proving the efficiency of the moving shoreline treatment. In addition, a demanding test involving irregular wave breaking over a submerged bar showed good agreement.

The Boussinesq-type model was also compared with an SPH model for a regular plunging breaking test. The latter proved superior by means of accuracy, especially in the surf zone. As expected, the intense free surface deformation caused by the plunging breaker is very well described by the SPH model due to its Lagrangian nature. However, the computational time for a simulation by such a model is typically very much higher than for a Boussinesq model. Hence, a computational efficiency analysis is needed to decide which model would be more suitable for each specific case.

The two-dimensional validation included two test cases. The first one referred to regular wave propagation over an elliptic shoal. Complex phenomena as the nonlinear diffraction and energy focusing behind the shoal were adequately reproduced. The second test involved oblique incidence of long-crested irregular waves on a sloping beach. The agreement was found reasonable since the spectra transformation and the energy transfer were acceptably estimated.

In conclusion, the Boussinesq-type model presented herein proved an efficient tool for simulating most of the nearshore phenomena such as shoaling, refraction, diffraction, wave breaking and run-up.

ACKNOWLEDGMENTS

The first author (G.K.) gratefully acknowledges the scholarship provided by the “Onassis Foundation”. He also acknowledges the support by the Danish Council for Strategic Research (DSF) under the project: Danish Coasts and Climate Adaptation - flooding risk and coastal protection (COADAPT), project no. 09-066869.

REFERENCES

Basco D.R. (1983). Surfzone currents. *Coast. Eng.*, 7 (4), 331-355.

Beji S. and Battjes J.A. (1994). Numerical simulation of nonlinear wave propagation over a bar. *Coast. Eng.*, 23 (1-2), 1-16.

Berkhoff J.C.W., Booij N., and Radder A.C. (1982). Verification of numerical wave propagation models for simple harmonic linear water waves. *Coast. Eng.*, 6 (3), 255–279.

Chen Q., Dalrymple R.A., Kirby J.T., Kennedy A.B., and Haller M.C. (1999). Boussinesq modeling of a rip current system. *J. Geophys. Res.*, 104 (C9), 20617-20637.

Chen Q., Kirby J.T., Dalrymple R.A., Kennedy A.B., and Chawla A. (2000). Boussinesq modeling of wave transformation, breaking and runup. II: 2D. *J. Waterw. Port Coast. Ocean Eng.*, 126 (1), 48-56.

Cox D.T., Kobayashi N., and Okayasu A. (1994). Vertical Variations of Fluid Velocities and Shear Stress in Surf Zones. *Proc. 24th Int. Conf. Coast. Eng.* (ed. B.L. Edge), ASCE, Kobe, Japan, pp. 98-112.

Dalrymple R.A. and Rogers B.D. (2006). Numerical Modeling of Water Waves with SPH Method. *Coast. Eng.*, 53 (2-3), 141-147.

Dingemans M.W. (1994). *Water wave propagation over uneven bottoms*. PhD thesis, Delft University of Technology.

Feddersen F., Guza R.T., Elgar S., and Herbers T.H.C. (2000). Velocity moments in alongshore bottom stress parameterizations. *J. Geophys. Res.*, 105 (C4), 8673-8686.

Gobbi M.F., Kirby J.T., and Wei G.E. (2000). A fully nonlinear Boussinesq model for surface waves. Part 2. Extension to $O(kh)^4$. *J. Fluid Mech*., 405, 181-210.

Gómez-Gesteira M., Rogers B.D., Dalrymple R.A., and Crespo A.J.C. (2010a). State-of-the-art of Classical SPH for Free-Surface Flows. *J. Hydraul. Res.*, 48, Extra Issue, 6-27.

Gómez-Gesteira M., Rogers B.D., Dalrymple R.A., Crespo A.J.C., and Narayanaswamy M. (2010b). *User Guide for the SPHysics Code v2.0*.

Hansen J.B. and Svendsen I.A. (1979). *Regular waves in shoaling water, experimental data*. Inst. Hydrodyn. Hydr. Eng., Series Paper 21.

Israeli M. and Orszag S.A. (1981). Approximation of radiation boundary conditions. *J. Comput. Phys.*, 41 (1), 115-135.

Karambas Th.V. and Koutitas C. (2002). Surf and swash zone morphology evolution induced by nonlinear waves. *J. Waterw. Port Coast. Ocean Eng.*, 128 (3), 102-113.

Karambas Th.V., and Memos C.D. (2009). Boussinesq model for weakly nonlinear fully dispersive water waves. *J. Waterw. Port Coast. Ocean Eng.*, 135 (5), 187-199.

Kennedy A.B., Chen Q., Kirby J.T., and Dalrymple R.A. (2000). Boussinesq modeling of wave transformation, breaking and runup. I: 1D. J. Waterw. *Port Coast. Ocean Eng.*, 126 (1), 39-47.

Klonaris G.Th., Memos C.D., and Drønen N.K. (2015). A higher order Boussinesq-type model integrating nearshore dynamics (to be submitted).

Kobayashi N., Agarwal A., and Bradley D.J. (2007). Longshore current and sediment transport on beaches. *J. Waterw. Port Coast. Ocean Eng.*, 133 (4), 296-304.

Madsen P.A., Bingham H.B., and Hua Liu (2002). A new Boussinesq model for fully nonlinear waves from shallow to deep water. *J. Fluid Mech*., 462, 1-30.

Madsen P.A., Murray R., and Sørensen O.R. (1991). A new form of the Boussinesq equations with improved linear dispersion characteristics. *Coast. Eng.*, 15 (4), 371-388.

Madsen P.A., and Schäffer H. A. (1998). Higher-order Boussinesq-type equations for surface gravity waves: derivation and analysis. *Philos. Trans. R. Soc. Lond.*, A 356, 3123-3181.

Madsen P.A., Sørensen O.R., and Schäffer H.A. (1997a). Surf zone dynamics simulated by a Boussinesq type model. Part I. Model description and cross-shore motion of regular waves. *Coast. Eng.*, 32 (4), 255-287.

Madsen P.A., Sørensen O.R., and Schäffer H.A. (1997b). Surf zone dynamics simulated by a Boussinesq type model. Part II: surf beat and swash oscillations for wave groups and irregular waves. *Coast. Eng.*, 32 (4), 289–319.

Makris C.V., Krestenitis Y.N., and Memos C.D. (2015a). SPH modelling of coherent structures and intermittent events in the surf zone of weak plungers. *Proc. of 36th IAHR World Congress*, The Hague, the Netherlands, 28th June – 3rd July 2015.

Makris C.V., Memos C.D., and Krestenitis Y.N. (2015b). Numerical modeling of surf zone dynamics under weak plunging breakers with SPH method. *Ocean Modelling* (under review).

Mei C.C. (1983). *The Applied Dynamics of Ocean Surface Waves*. J. Wiley and Sons, New York, 740 pp. (Corrected reprint, World Scientific, 1989).

Memos C.D., Karambas Th.V., and Avgeris I. (2005). Irregular wave transformation in the nearshore zone: experimental investigations and comparison with a higher order Boussinesq model. *Ocean Eng.*, 32 (11-12), 1465-1485.

Memos C.D., Klonaris G.Th., and Chondros M.K. (2015). On higher order Boussinesq-type wave models. *J. Waterw. Port Coast. Ocean Eng.* (under review).

Militello A., Reed C.W., Zundel A.K., Kraus. N.C. (2004). *Two-Dimensional Depth-Averaged circulation model M2D: version 2.0, Report 1, technical documentation and user's guide*. US Army Corps of Engineers, ERDC/CHL TR-04-2.

Monaghan J.J. (2005). Smoothed Particle Hydrodynamics. *Rep. Prog. Phys.*, 68, 1703-1759.

Nwogu O. (1993). Alternative form of Boussinesq equations for nearshore wave propagation. *J. Waterw. Port Coast. Ocean Eng*., 119 (6), 618-638.

Pedersen G., and Gjevik B. (1983). Run-up of solitary waves*. J. Fluid. Mech*., 135, 283-299.

Peregrine D.H. (1967). Long waves on a beach. *J. Fluid Mech*., 27 (4), 815-827.

Pope S.B. (2000). *Turbulent Flows*. Cambridge University Press, 802 pp.

Rakha K.A., Deigaard R., and Brøker I. (1997). A phase-resolving cross-shore transport model for beach evolution. *Coast. Eng.*, 31 (1-4), 231-261.

Schäffer H.A. and Madsen P.A. (1995). Further enhancements of Boussinesq-type equations. *Coast. Eng.*, 26 (1-2), 1-14.

Schäffer H.A., Madsen P.A., and Deigaard R. (1993). A Boussinesq model for waves breaking in shallow water. *Coast. Eng*., 20 (3-4), 185-202.

Shapiro R. (1970). Smoothing, filtering, and boundary effects. *Rev. Geophys. and Space Phys.*, 8 (2), 359-386.

Stansby P.K. and Feng T. (2005). Kinematics and depth-integrated terms in surf zone waves from laboratory measurements. *J. Fluid Mech.*, 529, 279–310.

Synolakis C.E. (1987). The runup of solitary waves. *J. Fluid Mech.*, 185, 523–545.

Tao J. (1983). *Computation of wave run-up and wave breaking*. Internal Report, Danish Hydraulic Institute, 40 pp.

Tao J. (1984). Numerical modelling of wave runup and breaking on the beach. *Acta Oceanol. Sin.*, 6(5), 692-700, in Chinese.

Veeramony J. and Svendsen I.A. (2000). The flow in surf-zone waves. *Coast. Eng.*, 39 (2-4), 93-122.

Violeau D. (2012). *Fluid Mechanics and the SPH Method - Theory and Applications*. Oxford University Press, 616 pp.

Wei G. and Kirby J.T. (1995). Time-dependent numerical code for extended Boussinesq equations. *J. Waterw. Port Coast. Ocean Eng.*, 121 (5), 251-261.

Wei G., Kirby J.T., Grilli S.T., and Subramanya R. (1995). A fully non-linear Boussinesq model for surface waves. Part 1. Highly non-linear unsteady waves. *J. Fluid Mech.*, 294, 71–92.

Wei G., Kirby J.T., and Sinha A. (1999). Generation of waves in Boussinesq models using a source function method. *Coast. Eng.*, 36 (4), 271-299.

Zelt J.A. (1991). The run-up of nonbreaking and breaking solitary waves. *Coast. Eng.*, 15 (3), 205-246.

Zhan J.M., Li Y.S., Wai O.W.H. (2003). Numerical modeling of multi-directional irregular waves incorporating 2-D numerical wave absorber and subgrid turbulence. *Ocean Eng.*, 30 (1), 23-46.

Zlatev Z., Berkowicz R., and Prahm L.P. (1984). lmplementation of a variable stepsize variable formula method in the time-integration part of a code for treatment of long-range transport of air pollutants. *J. Comput. Phys.*, 55 (2), 278-301.